Supplementary figures to: "Modeling the vertical soil organic matter profile using $^{210}Pb_{ex}$ measurements and Bayesian inversion"

Maarten C. Braakhekke, Thomas Wutzler, Markus Reichstein, Jens Kattge, Christian Beer, Marion Schrumpf, Ingo Schöning, Marcel R. Hoosbeek, Bart Kruijt, and Pavel Kabat

List of Figures

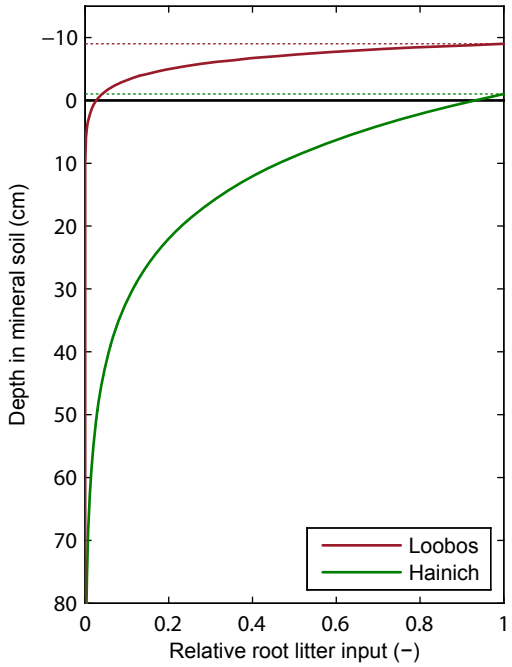

Figure 1: The vertical root litter input distribution as used in the model simulations for Loobos ($\beta = 0.4\,\mathrm{m}^{-1}$) and Hainich ($\beta = 0.07\,\mathrm{m}^{-1}$). The dotted lines represent the approximate top of the F horizon for both sites.

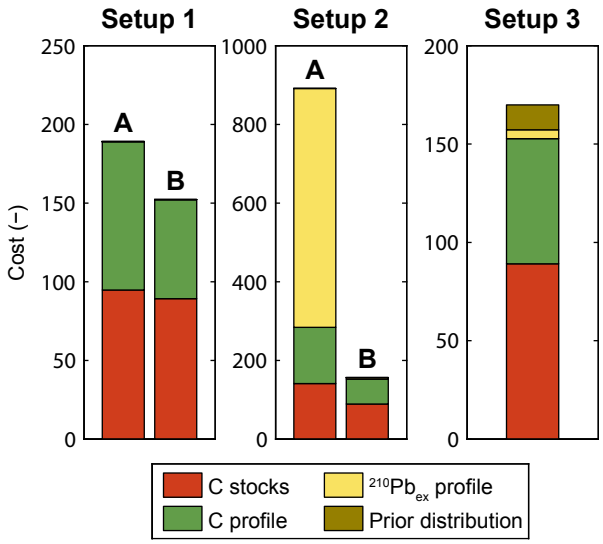

Figure 2: The contribution of the different observations to the total cost for the different optimization setups for Loobos. Depicted costs are for the sample with the lowest total cost.

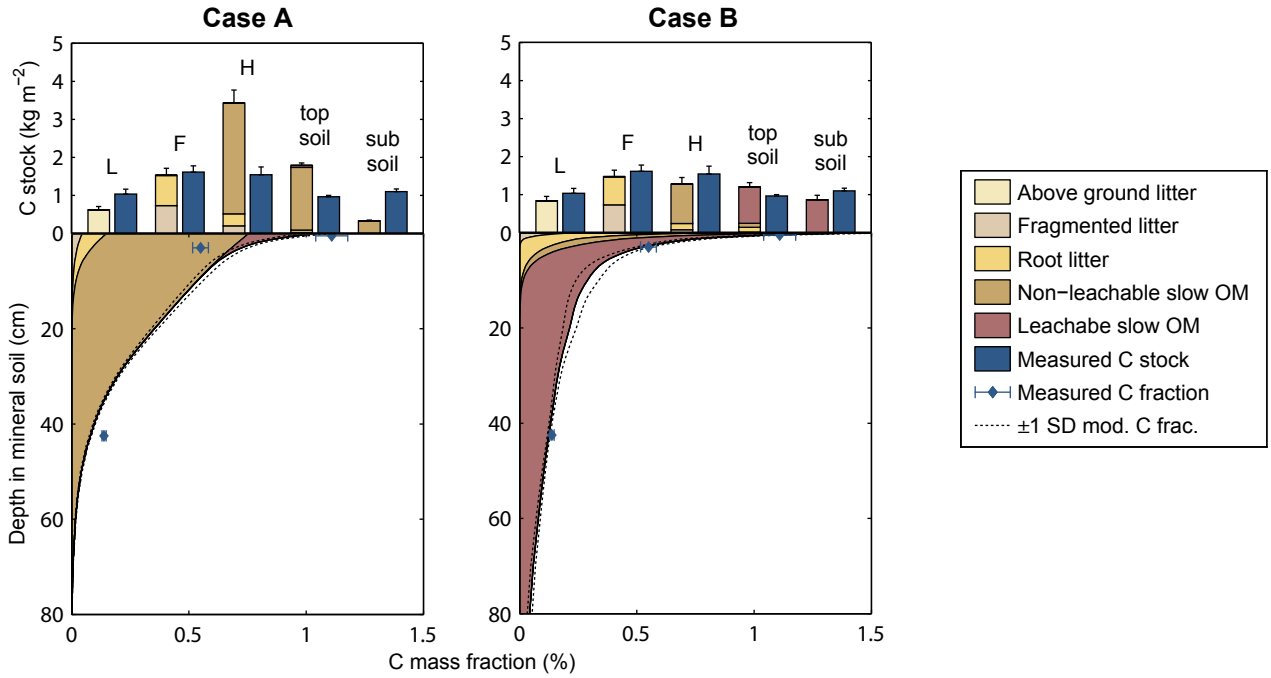

Figure 3: Measured and modeled carbon stocks (topsoil: 0–30 cm; subsoil: >30 cm) and mass fractions for Loobos. Model results are from forward Monte Carlo runs based on posterior samples from the two cases of optimization setup 2 (including $^{210}Pb_{ex}$ and with weak priors). Depicted stocks and fractions are averages. Errorbars denote one standard error of the mean for the measurements and one standard deviation for the model results.

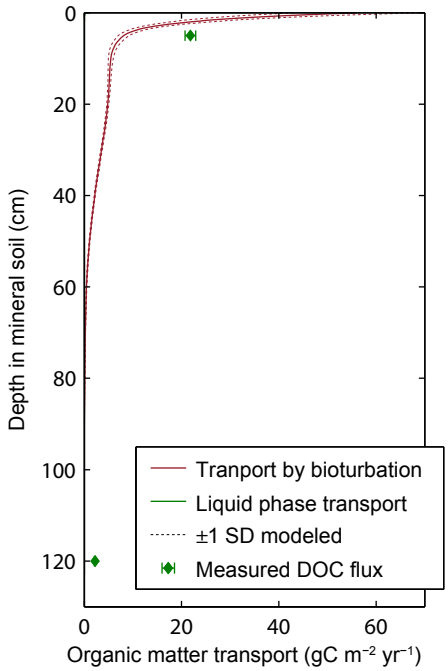

Figure 4: Modeled vertical transport fluxes for Loobos, from forward Monte Carlo simulations based on posterior samples of optimization setup 2, case A. The depicted fluxes are averages for the last simulation year. The dashed line indicates the standard deviation over the Monte Carlo ensemble. Measured DOC fluxes were taken from Kindler et al. (2011).

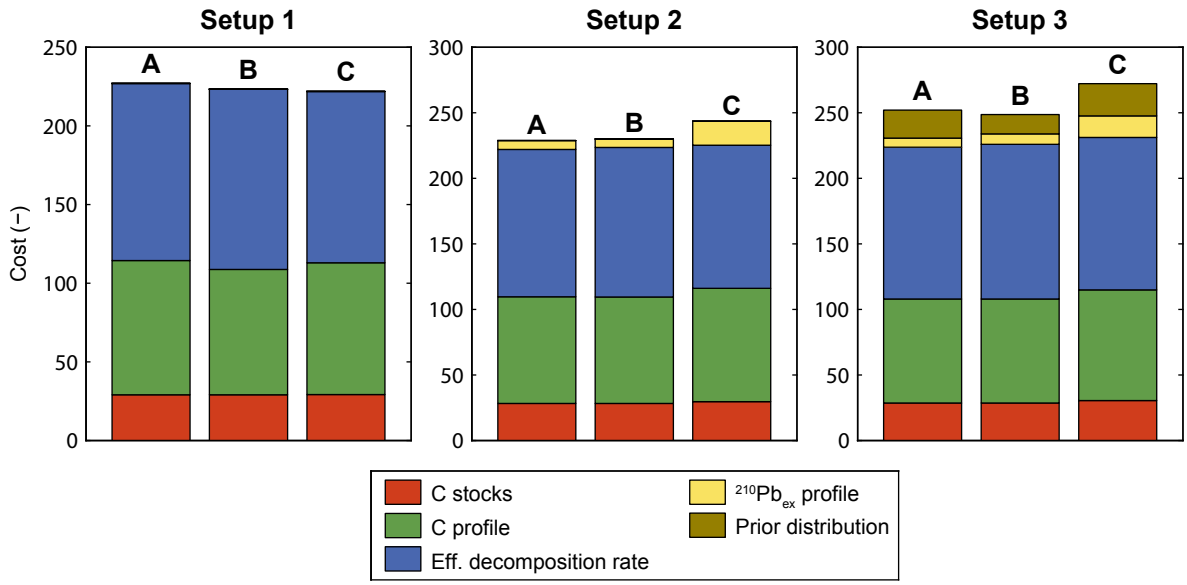

Figure 5: The contribution of the different observations to the total cost for the different optimization setups for Hainich. Depicted costs are for the sample with the lowest total cost.

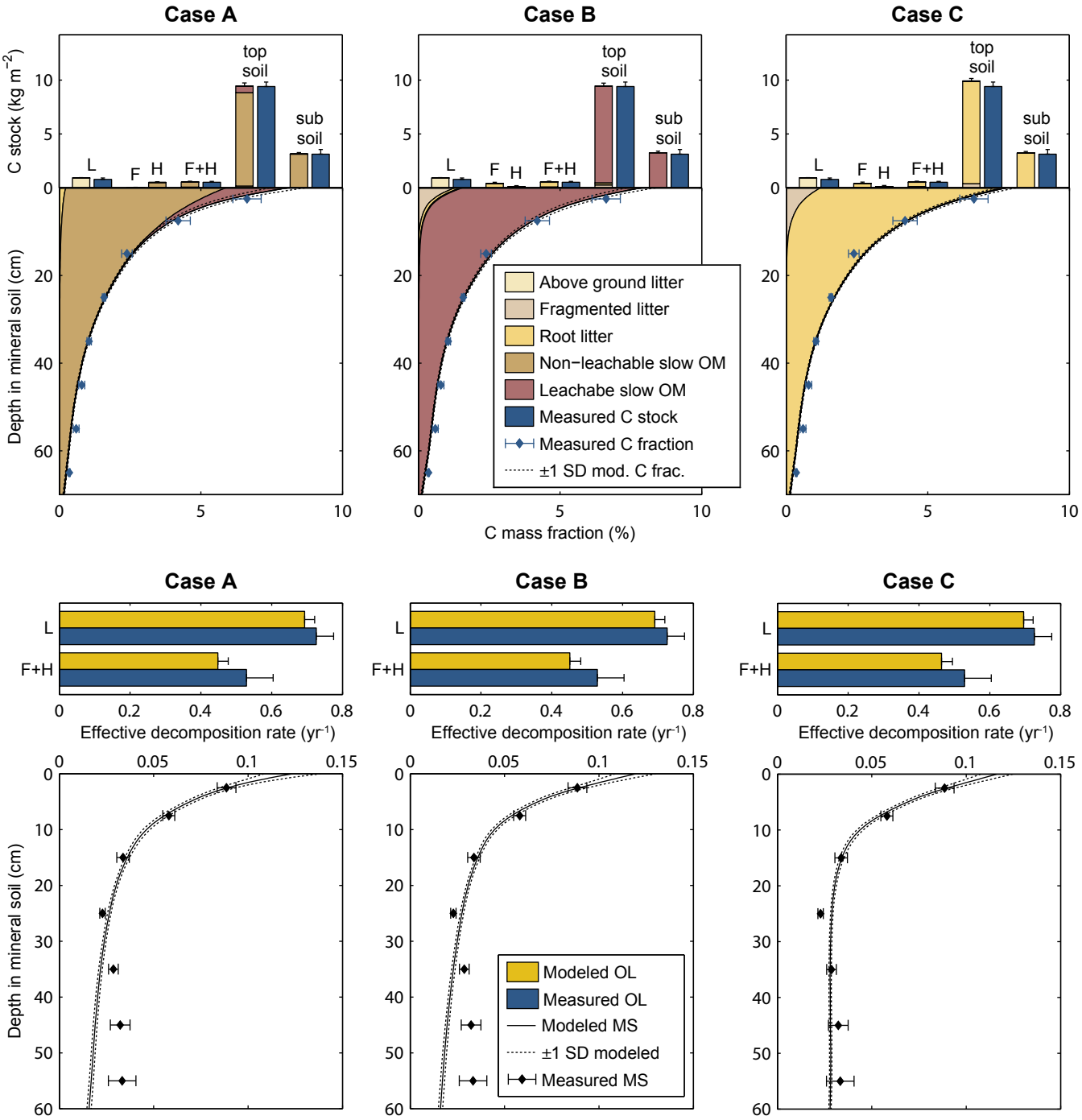

Figure 6: Results from forward Monte Carlo simulations for Hainich based on posterior samples from the three cases of optimization 2 (including $^{210}Pb_{ex}$ and with weak priors). Top: measured and modeled carbon stocks (topsoil: 0–30 cm; subsoil: >30 cm) and mass fractions; bottom: measured and modeled effective decomposition rates. All depicted values are averages. Errorbars denote one standard error of the mean for the measurements and one standard deviation for the model results.

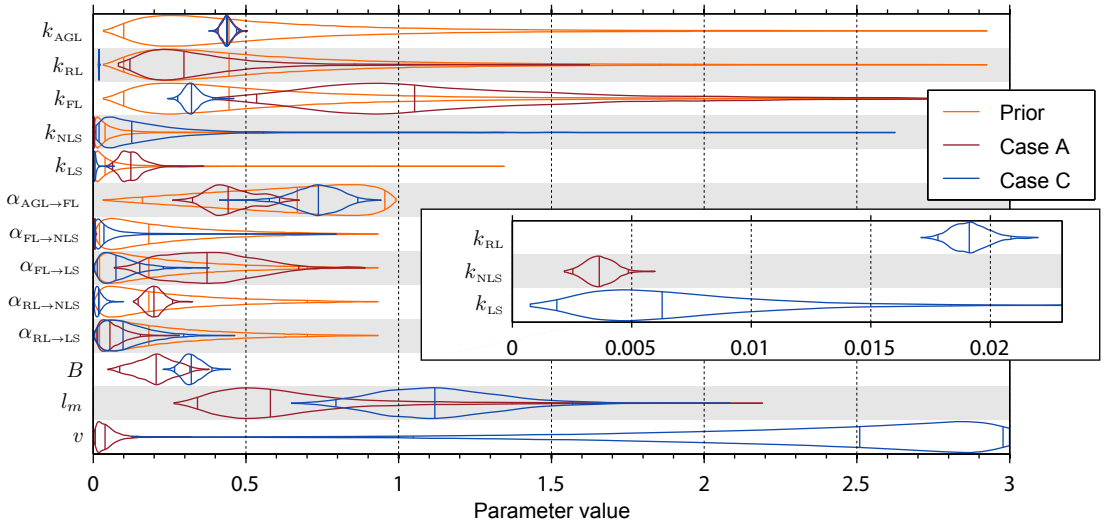

Figure 7: Violin plots of the prior and posterior distributions for Hainich, optimizations 3, cases A and C. The violins indicate the marginal distributions for each parameter. The three vertical lines inside the violins indicate the median and the 95 % confidence bounds.

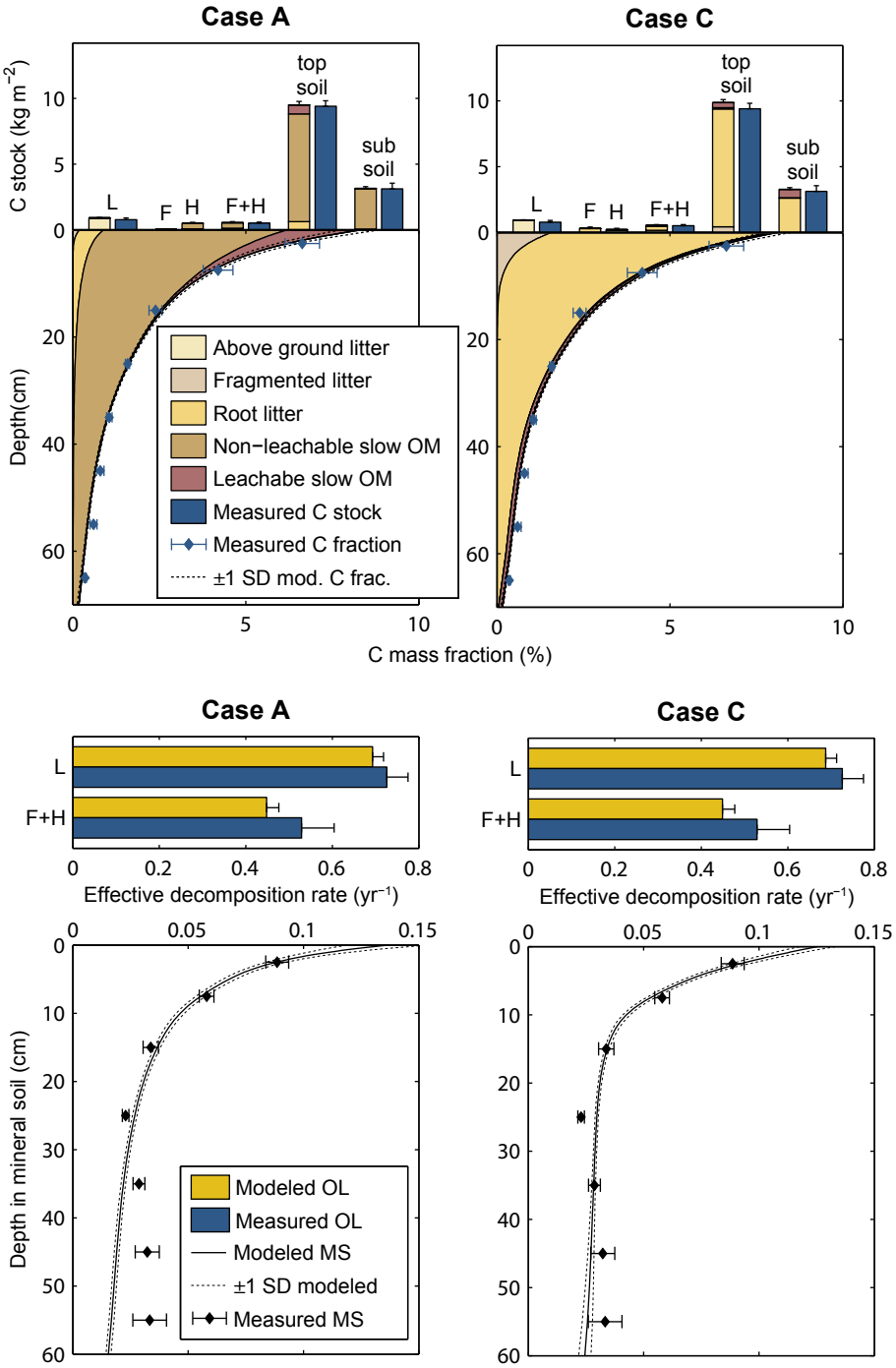

Figure 8: Results from forward Monte Carlo simulations for Hainich based on posterior samples optimization 3, cases A and C (including $^{210}Pb_{ex}$ and with strong priors). Top: measured and modeled carbon stocks (topsoil: 0–30 cm; subsoil: >30 cm) and mass fractions; bottom: measured and modeled effective decomposition rates. All depicted values are averages. Errorbars denote one standard error of the mean for the measurements and one standard deviation for the model results.

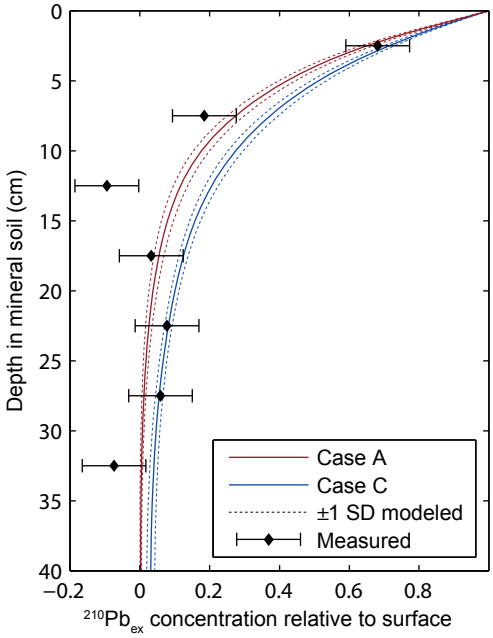

Figure 9: Measured and modeled $^{210}Pb_{ex}$ profile for Hainich. Modeled results are from forward Monte Carlo runs based on posterior samples of optimization setup 3, cases A and B (including $^{210}Pb_{ex}$ and with weak priors).

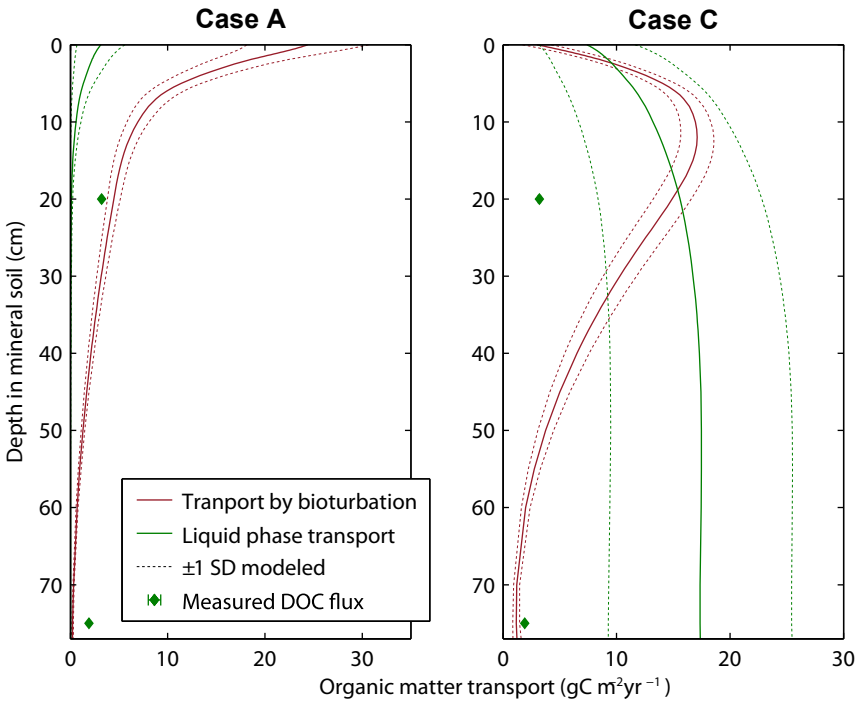

Figure 10: Modeled vertical transport fluxes for Hainich, from forward Monte Carlo simulations based on posterior samples of optimization setup 3, cases A and C. The depicted fluxes are averages for the last simulation year. The dashed line indicates the standard deviation over the Monte Carlo ensemble. Measured DOC fluxes were taken from Kindler et al. (2011).

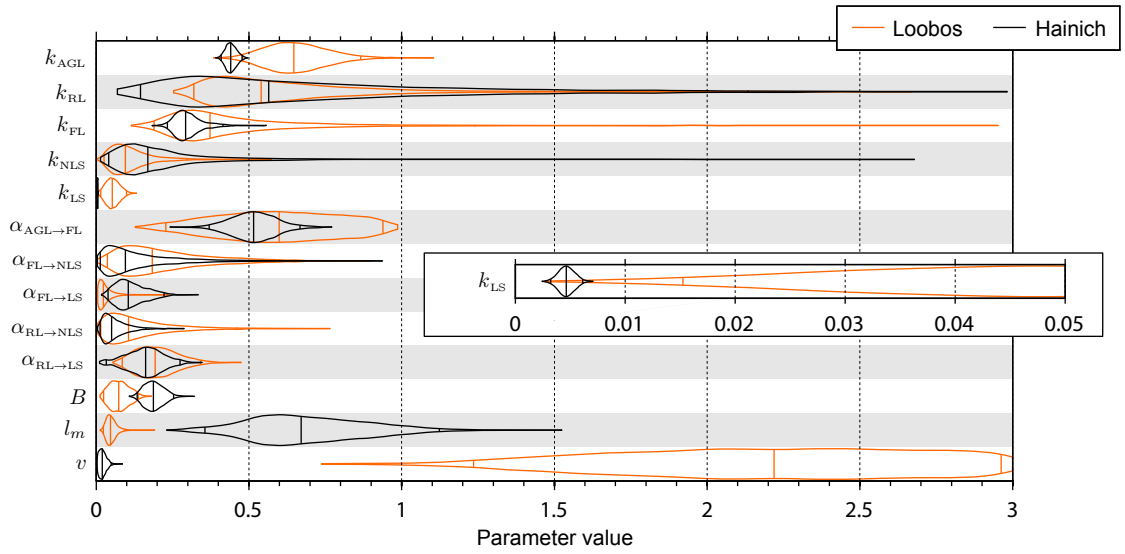

Figure 11: Violin plots of the posterior distributions for optimization setup 3 for Loobos and Hainich (case B). The violins indicate the marginal distributions for each parameter. The three vertical lines inside the violins are the median and the 95 % confidence bounds.

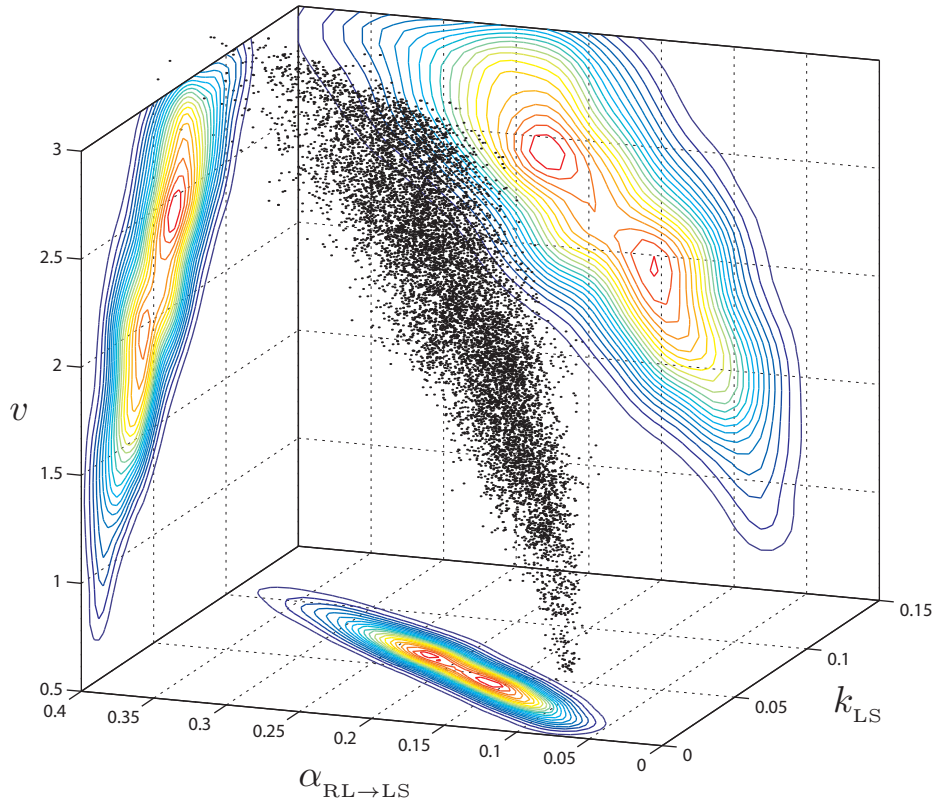

Figure 12: 3D scatter plot of the MCMC sample for the parameters k_{AOM}, $\alpha_{\mathrm{RL}\to\mathrm{AOM}}$, and v, for Loobos, optimization 3. The contour plots on the axis planes depict lines of equal probability density for the marginal bivariate distributions. [a]

[a] The cloud of points is sometimes invisible in Adobe Reader. If so, try zooming in or out.

References

Kindler, R., Siemens, J., Kaiser, K., Walmsley, D. C., Bernhofer, C., Buchmann, N., Cellier, P., Eugster, W., Gleixner, G., Grunwald, T., Heim, A., Ibrom, A., Jones, S. K., Jones, M., Klumpp, K., Kutsch, W., Larsen, K. S., Lehuger, S., Loubet, B., McKenzie, R., Moors, E., Osborne, B., Pilegaard, K., Rebmann, C., Saunders, M., Schmidt, M. W. I., Schrumpf, M., Seyfferth, J., Skiba, U., Soussana, J. F., Sutton, M. A., Tefs, C., Vowinckel, B., Zeeman, M. J., and Kaupenjohann, M.: Dissolved carbon leaching from soil is a crucial component of the net ecosystem carbon balance, Global Change Biology, 17, 1167–1185, 2011.